PNAS
www.pnas.org

Supplementary Information for

A physiologic rise in cytoplasmic calcium ion signal increases pannexin1 channel activity via a c-terminus phosphorylation by CaMKII

Ximena López[1], Nicolás Palacios-Prado[1,2], Juan Güiza[3], Rosalba Escamilla[1,2], Paola Fernández[2], José L. Vega[3] Maximiliano Rojas[4], Valeria Marquez-Miranda[2,6], Eduardo Chamorro[5], Ana M. Cárdenas[2], María Constanza Maldifassi[2], Agustín D. Martínez[2], Yorley Duarte[2,4], Fernando D. González-Nilo[2,4] and Juan C. Sáez[1,2]*

*corresponding author Juan C. Saez.

Email: juancarlos.saez@uv.cl

This PDF file includes:

Figures S1 to S12
Tables S1 to S2
Legends for Movies S1 to S2

Other supplementary materials for this manuscript include the following:

Movies S1 to S2

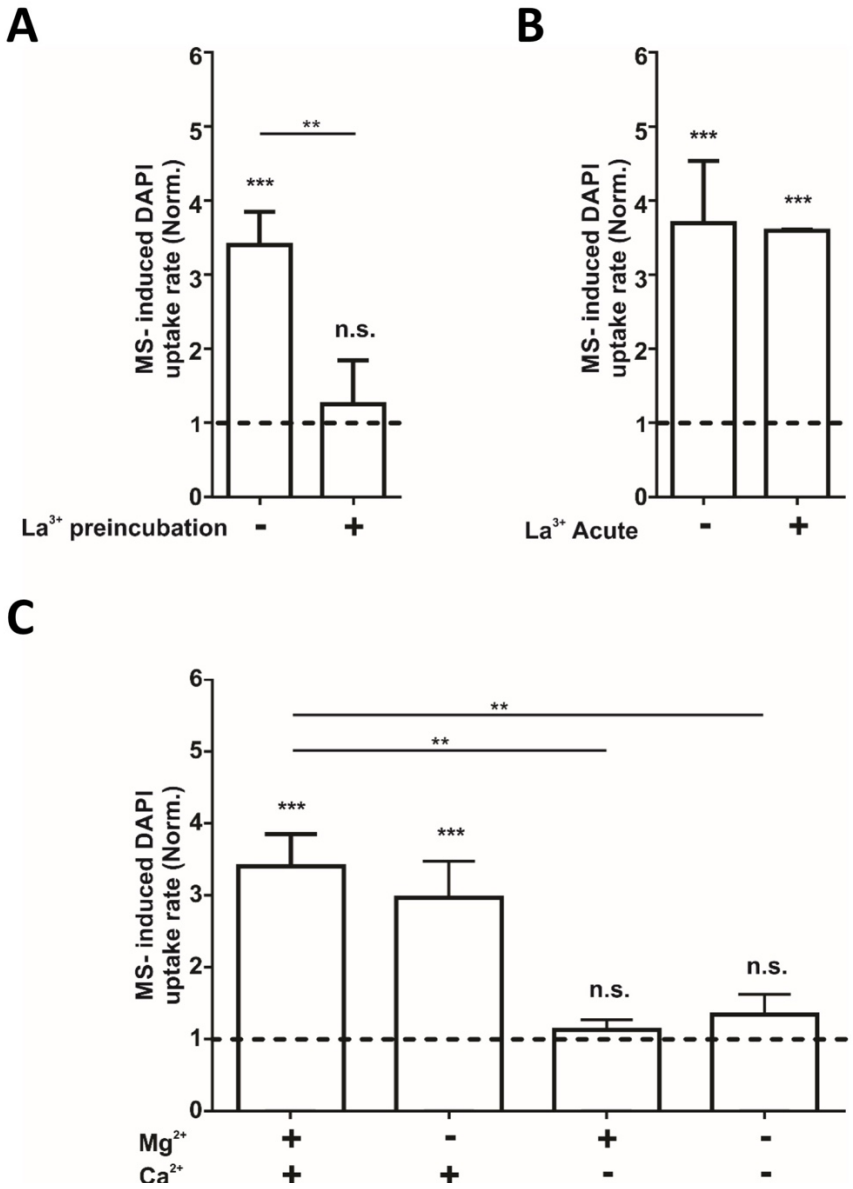

Figure S1. Membrane stretch depends on the activity of a known mechanical stretch activated channel and the presence of extracellular Ca^{2+}. (***A***) DAPI uptake rate normalized (Norm.) with respect to baseline uptake in HeLa rPanx1-EGFP cells subjected to MS, preincubated or not with La^{3+}. (***B***) DAPI uptake rate normalized with respect to baseline uptake in HeLa rPanx1-EGFP cells subjected to MS and subsequently treated or not with 200 μM La^{3+}. (***C***) DAPI uptake rate normalized with respect to baseline uptake in the presence of both divalent cations, absence of each one, and absence of both. Each value in ***A***, ***B*** and ***C*** corresponds to the mean ± standard error of a total of three to four independent experiments. * p <0.05; ** p <0.005, *** p <0.001 and n.s. = non-significant compared to the basal value represented with a dotted line.

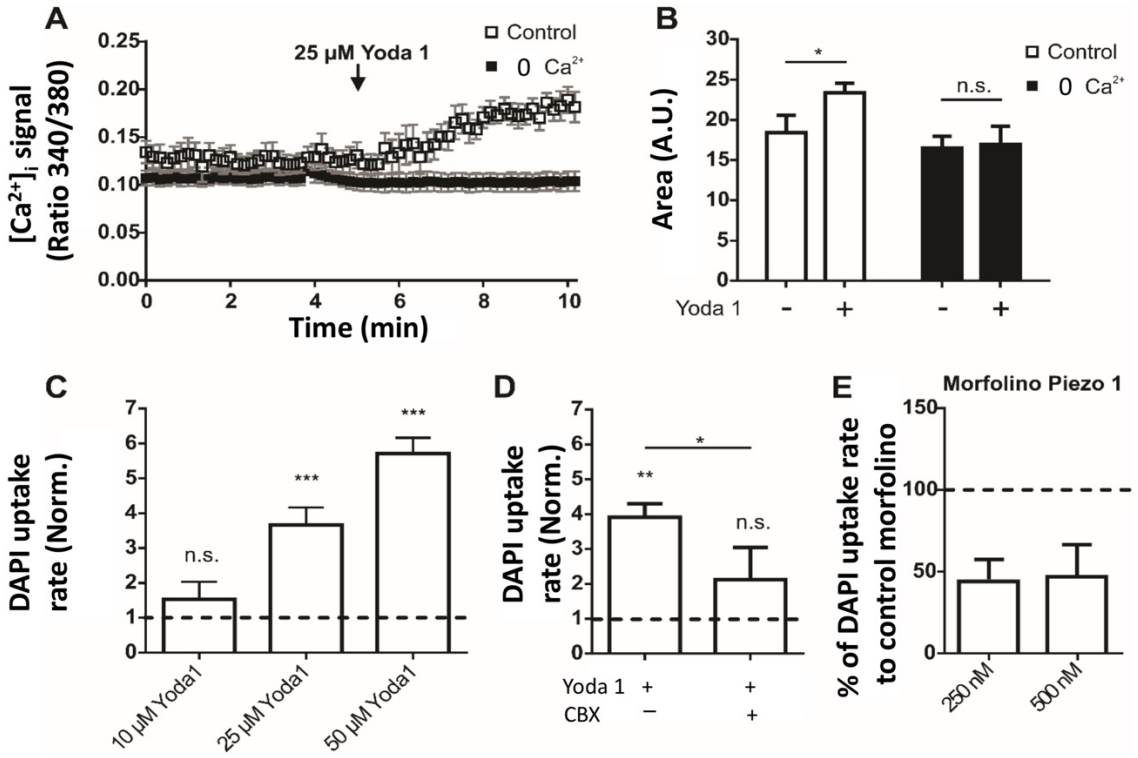

Figure S2. Piezo 1 channel activation increases the activity of rPanx1-EGFP channels. (***A***) Image of the representative Ca^{2+} signal measured as the ratio of emissions to F340/F380 in HeLa rPanx1 cells preloaded with FURA-2AM, exposed or not to extracellular Ca^{2+}, and treated with 25 µM Yoda1 at the time indicated by the arrow. (***B***) Average area under the curve of three independent experiments as shown in ***A***. (***C-D***) DAPI uptake rate normalized with respect to baseline uptake in HeLa rPanx1-EGFP cells treated with different concentrations of Yoda1 (***C***), and with 25 µM Yoda1 and subsequently with 10 µM CBX (***D***). (***E***) DAPI uptake rate of HeLa rPanx1 cells subjected to MS and transfected with 250 or 500 nM morpholino against Piezo 1 (Morpholino against Piezo 1), relative to the DAPI uptake rate of HeLa rPanx1 cells subjected to MS and transfected with 250 or 500 nM control morpholino, respectively. Each value in ***B***, ***C***, ***D*** and ***E*** corresponds to the mean ± standard error of three independent experiments. * p <0.05; ** p <0.005 and *** p <0.001, and n.s = non-significant.

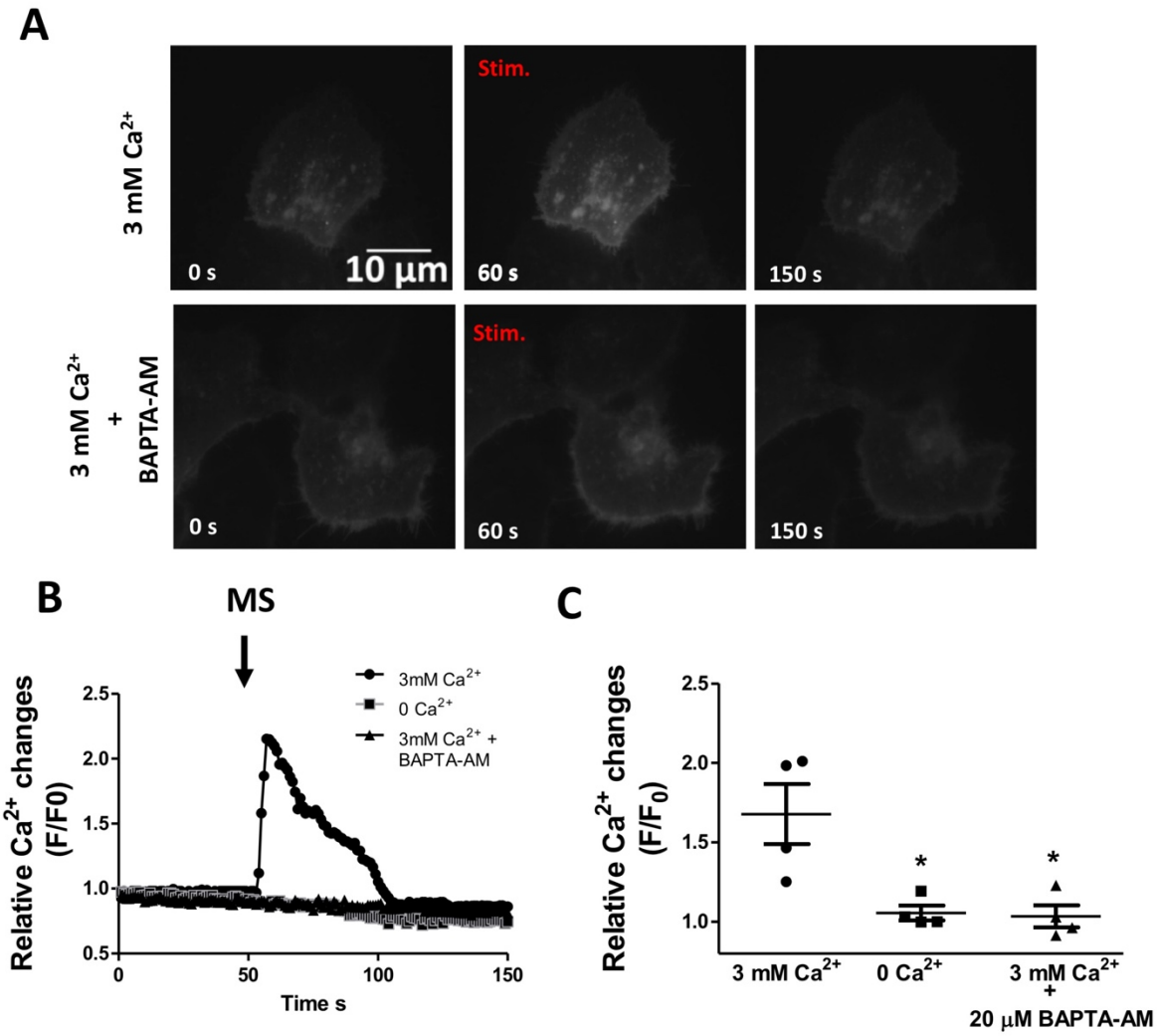

Figure S3. Membrane stretch triggers sub-membrane Ca^{2+} rises in Hela cells. (***A***) Representative images of Hela cells expressing Lck-GCaMP3 before and during MS. Top panel, stimulation achieved in the presence of 3 mM Ca^{2+}. In bottom panel, stimulation done in cells pre-incubated with 20 µM of BAPTA-AM and in the presence of 3 mM Ca^{2+}. (***B***) The relative fluorescence values were calculated as the F/F_0 ratio to represent the relative Ca^{2+} sub-membrane levels. Each dot represents averaged F/F_0 maximum values from four independent experiments, wherein submembrane areas of 5-6 cells were analyzed per coverslip. Horizontal lines indicate mean, and whiskers indicates the standard error. One-way ANOVA test with Bonferroni post hoc test. * $p < 0.05$.

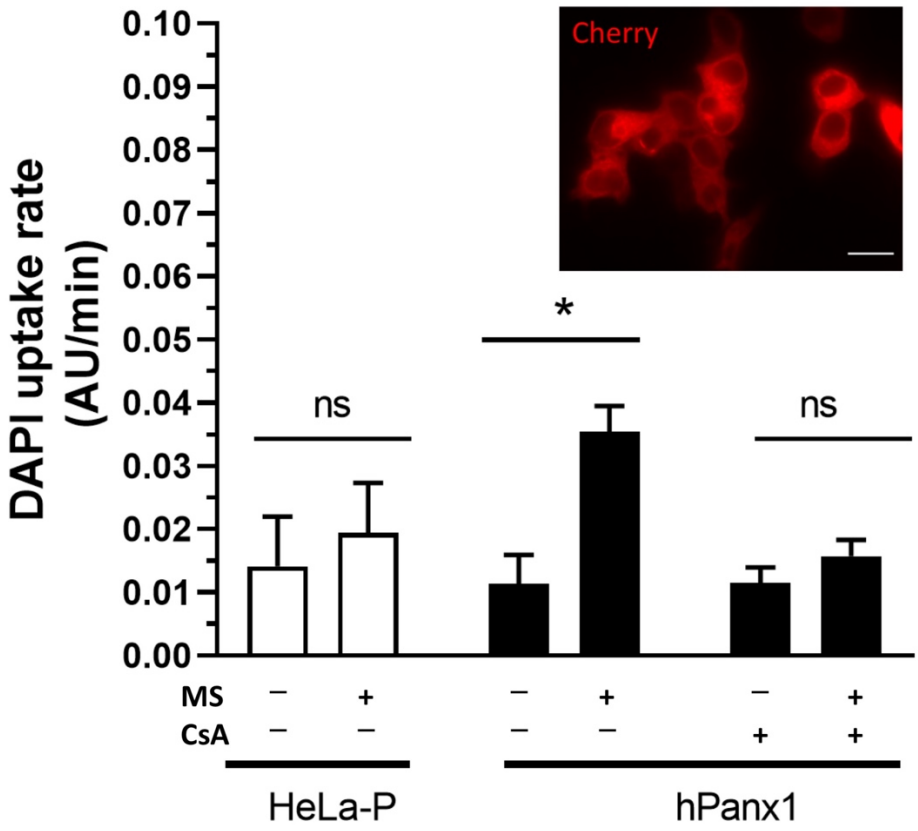

Figure S4. Response to membrane stretch of human Panx1 based channels. Evaluation of DAPI permeability in HeLa-parental cells (HeLa-P) and HeLa cells transiently transfected with hPanx1-Cherry and subjected to membrane stretch (MS) in presence or absence of 50 µg/mL cyclosporin A (CsA). The inset shows expression of hPanx1-Cherry (red) in transfected HeLa cells. Each value represent the average ± standard error. Scale bar = 20 µm. *p= 0.033, n.s. = non-significant. *n*=4, values were compared to basal conditions.

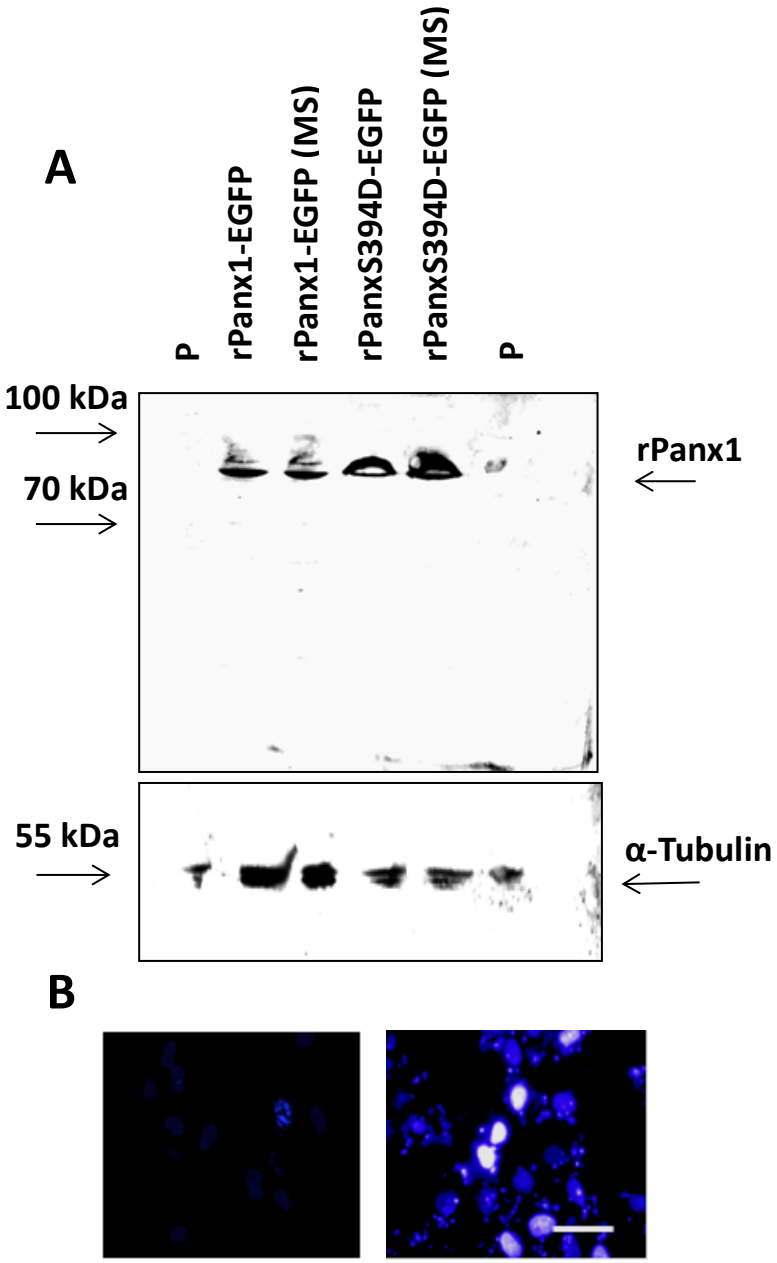

Figure S5. Western blot detection of rPanx1-EGFP polypeptides in cells subjected to membrane stretch. (***A***) Western blot detection of rPanx1-EGFP reactive polypeptides using and antibody directed to the C-terminal domain. Note that anti-Panx1 antibody recognized bands with similar intensity and electrophoretic mobility in lanes corresponding to rPanx1-EGFP or rPanx1394-EGFP under basal conditions or after membrane stretch (MS) and no reactivity in HeLa-parental cells (P). No proteolytic products were detected after MS treatment. α-Tubulin was developed as loading control. Representative western blot detection (n = 2). (***B***) Representative images of DAPI fluorescence in HeLa cell cultures transfected with rPanx1-EGFP before (left) and after (right) MS stimulation. Note that several cells show DAPI uptake after MS stimulation.

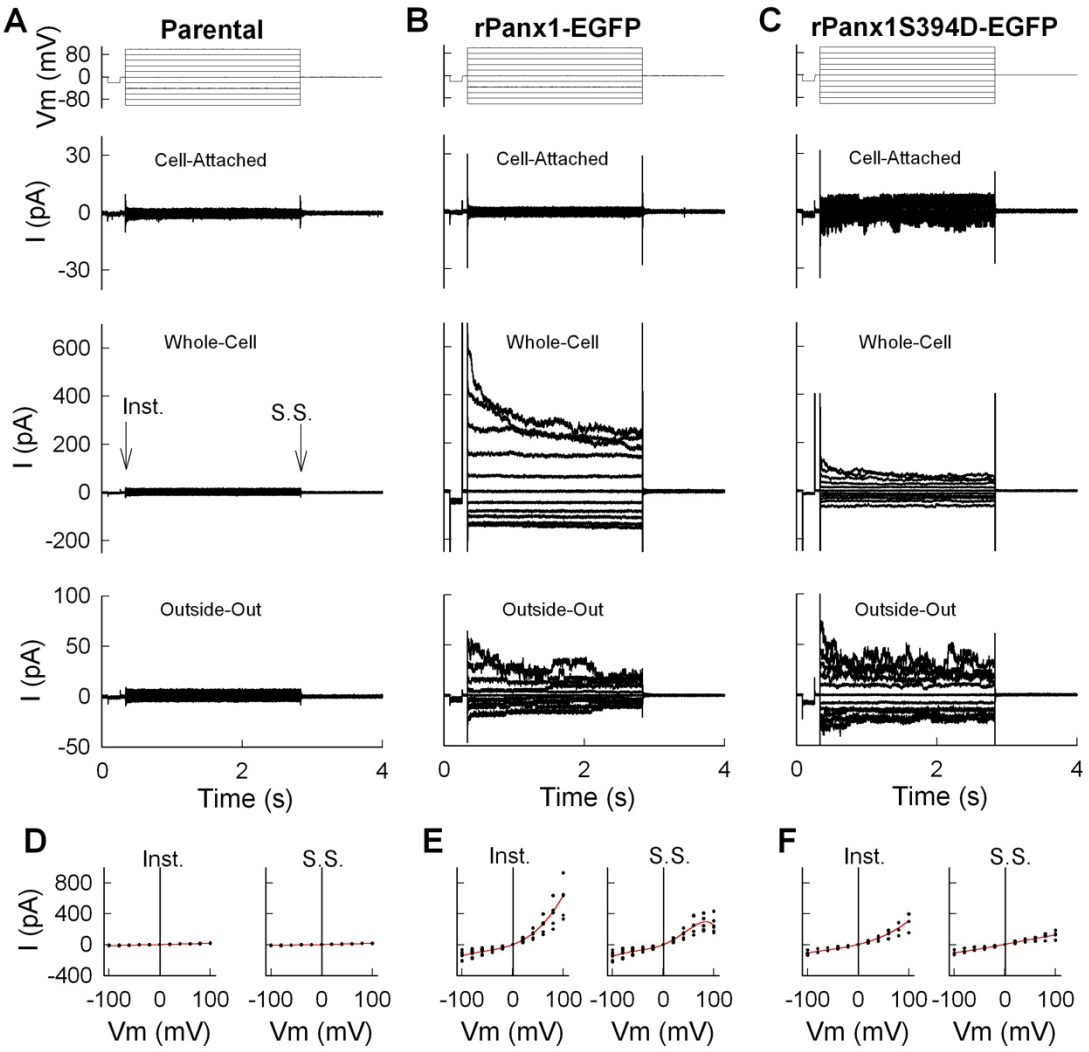

Figure S6. Patch-clamp recordings of rPanx1-EGFP and rPanx1S394D-EGFP channels in cell-attached, whole-cell and outside-out configurations. (***A-C***) Representative current traces obtained in cell-attached, whole-cell, and outside-out configurations from HeLa parental (***A***), HeLa cells expressing rPanx1-EGFP (***B***) or rPanx1S394D-EGFP (***C***) recorded in response to stepwise voltage pulses from -100 to +100 mV applied via 20 mV increments (upper traces). (***D-F***) Instantaneous (inst.) and steady-state (S.S.) current-voltage relationships for macroscopic currents recorded in whole-cell mode in Hela parental (***D***; *n*= 5), HeLa cells expressing rPanx1-EGFP (***E***; *n*= 7), or rPanx1S394D-EGFP (***F***; *n*= 4). All data points were fitted with a third order linear regression (red).

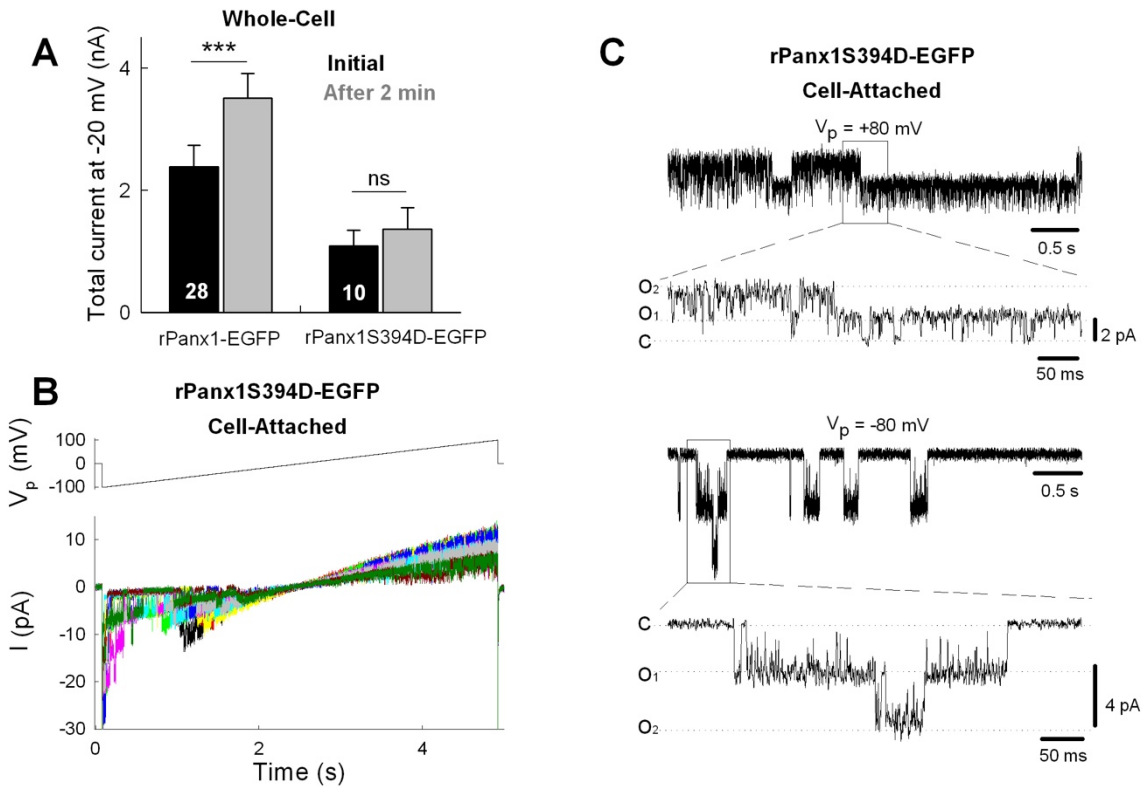

Figure S7. Single channel currents of rPanx1S394D-EGFP channels in cell-attached mode. (***A***) Average total current measured at -20 mV in whole-cell configuration for rPanx1-EGFP and rPanx1S394D-EGFP expressing cells. Averages and Standard errors were calculated at the beginning of the experiment (initial) and after 2 min of recording. Numerals in each column indicates number of independent experiments (***B***) Representative cell-attached recordings of single channel currents from HeLa cells expressing rPanx1S394D-EGFP in response to voltage ramps from -100 mV to 100 mV. The simultaneous activity of four functional rPanx1S394D-EGFP channels were recorded in the same patch. Color traces indicate different current sweeps from the same experiment and voltage ramp protocol. (***C***) Representative cell-attached recordings from HeLa cells expressing rPanx1S394D-EGFP at potential (V_p) +80 mV and -80 mV showing transitions between closed and open states. C, closed state; O_1, open-state channel 1; O_2, open-state channel 2.

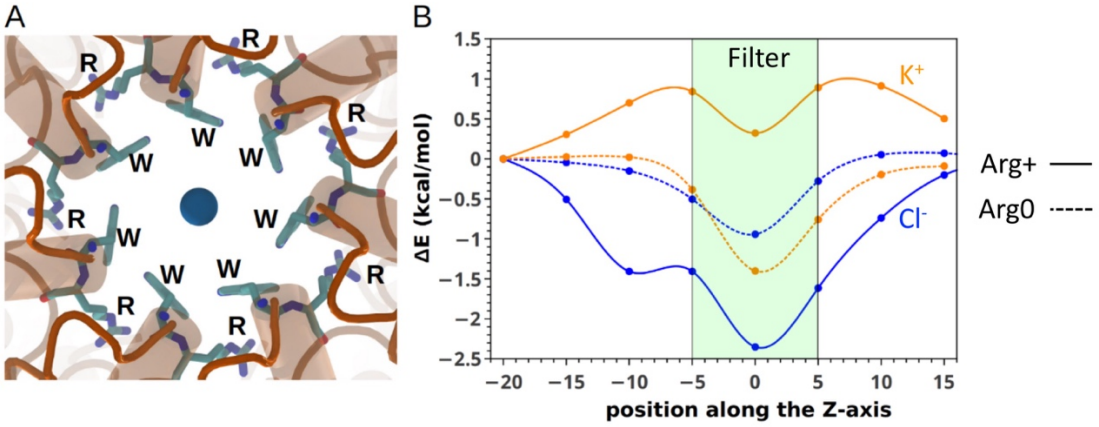

Figure S8. Arginine-Tryptophan conformation in the selectivity filter promotes the traslocation of anionic and also cationic species. (***A***) Conformation of Arg 75 and Trp 74 residues in the selectivity filter stabilized through cation-π interactions. (**B**) Quantum mechanical calculations of the passage of both Cl^- (blue) and K^+ ions (orange) along the central axis of the selectivity filter. The filter region is represented with a green bar. Two protonation states for Arg were considered: protonated (Arg+, solid lines) and neutral (Arg0, dotted lines). The Arg+ conditions shows that Cl^- ions are stabilized through anion-π interaction with the Trp residues, while at the same time the Arg residues contribute to generate an electropositive environment that stabilizes the anion about 2.0 kcal/mol at the filter region, compared to the position in the extracellular region ($z < -5$). Whereas, the K^+ ion energy profile is slightly higher in energy but still stable through a cation-π interaction. At Arg0 conditions, in absence of a higher electrostatic polarization state at the filter region, both Cl^- and K^+ ions can be attracted by the pore.

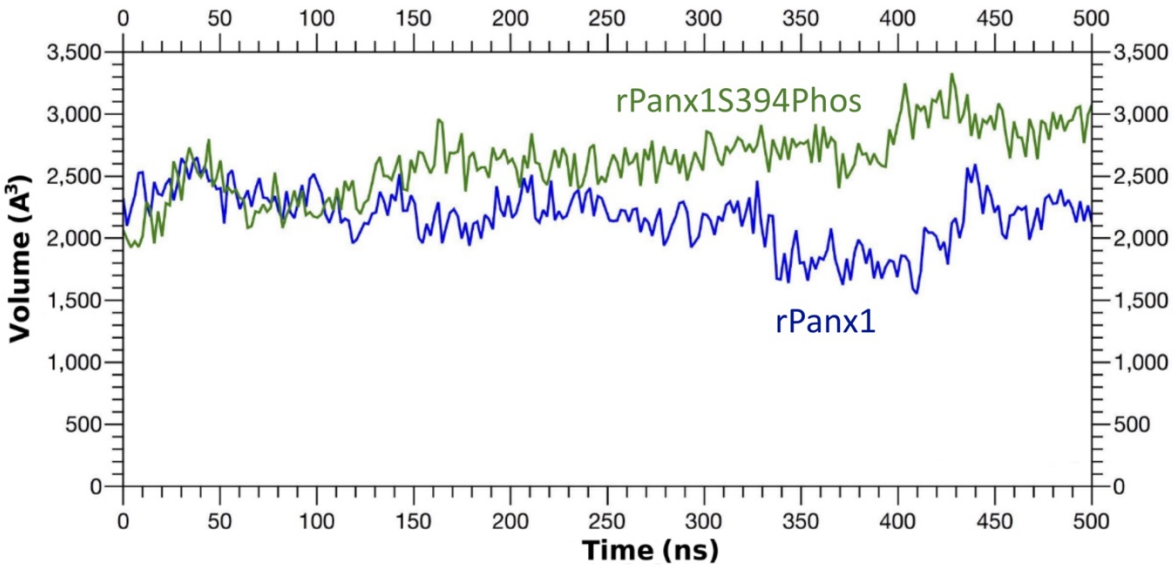

Figure S9. Phosphorylation of S394 residue promotes an increase of lateral cavity size. Volume of a lateral tunnel or cavity obtained along the molecular simulations at 0 mV. Cavity of the rPanx1 (blue) conserves it volume near 2,300 Å^3, while the cavity of rPanx1S394Phos (green) increases its volume until reaches ~3,000 Å^3.

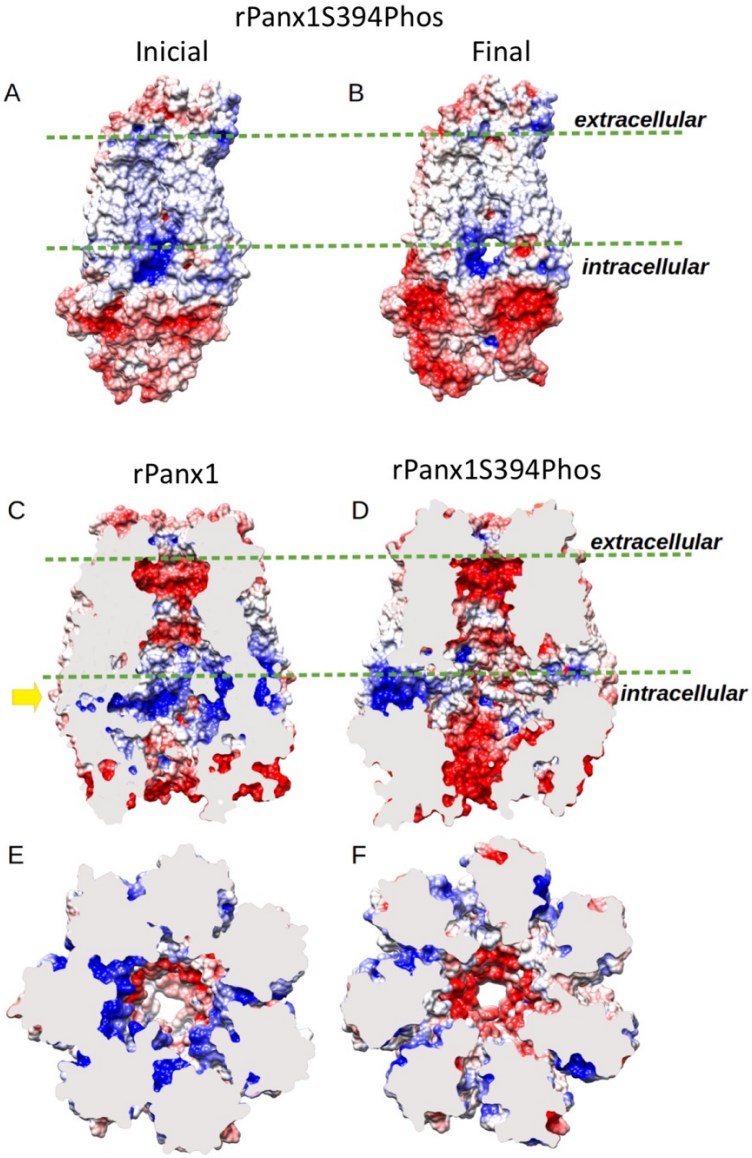

Figure S10. Phosphorylation of S394 residue promotes changes in the electrostatic potential of rPanx1 channel. Electrostatic potential maps of rPanx1 non-phosphorylated and phosphorylated by CaMKII. Lateral view of the electrostatic surface potential of the initial (***A***) and final (***B***) state of two monomers of S394Phos system. The increase of the size of the lateral tunnel in the final state is observed. Longitudinal section of the electrostatic surface map of Panx1 non-phosphorylated (***C***) and phosphorylated in S394Phos (***D***) obtained at 500 ns of the simulations at 0 mV. The cavity at the level of the lateral tunnel (depicted with a yellow arrow) appears electrostatically positive, being this effect enhanced in WT channel. Electrostatic potential map section, parallel to the axis pore, obtained at the level of the lateral tunnel for Panx1 non-phosphorylated (***E***) and phosphorylated in S394Phos (***F***). Scale bar used for maps: -5 kT/e to +5 kT/e; red representing negative potentials and blue representing negative positive potentials.

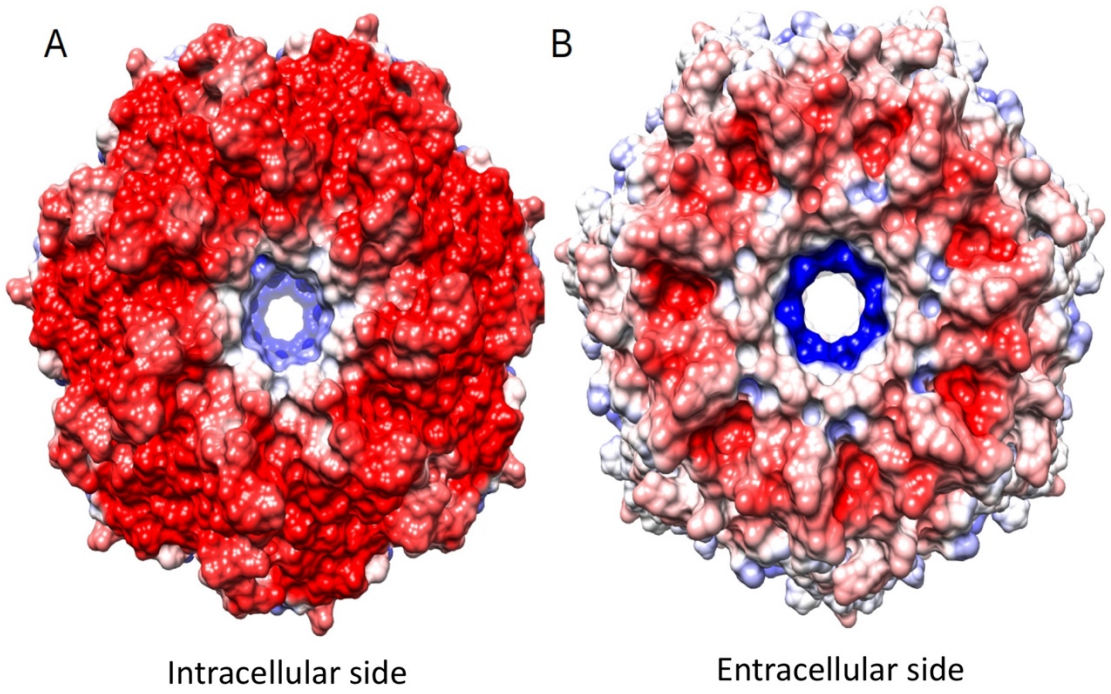

Figure S11. Intracellular and extracellular view of the electrostatic potential of rPanx1S394Phos channel. Electrostatic potential maps of (***A***) intracellular side and (***B***) extracellular side of rPanx1S394Phos channel. Scale bar used for maps: -5 kT/e to +5 kT/e; red representing negative potentials and blue representing positive potentials.

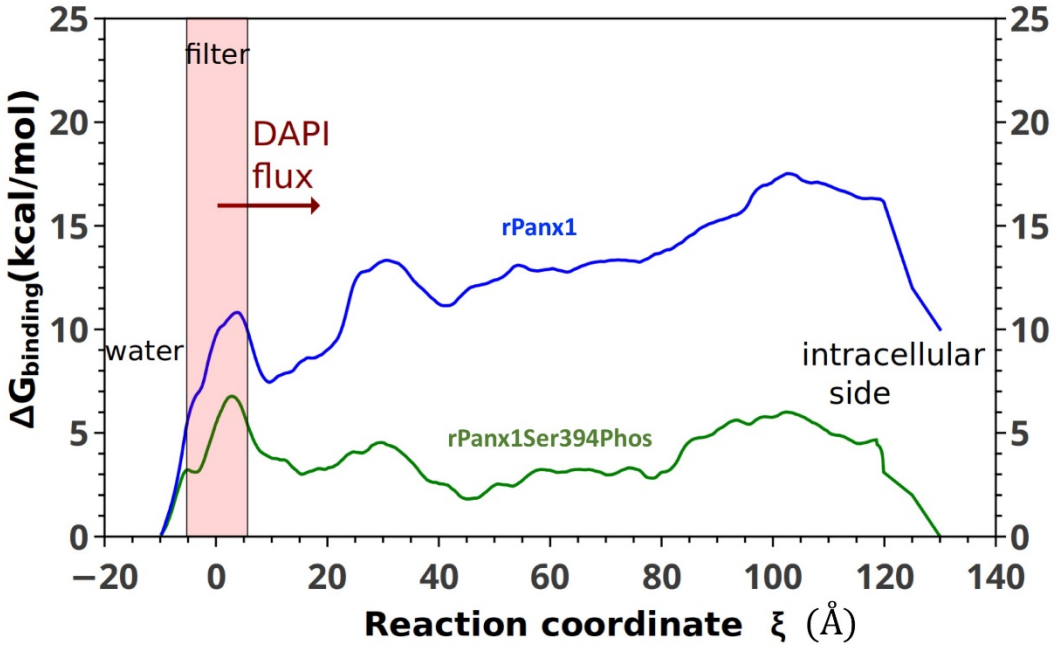

Figure S12. Phosphorylation of S394 residue promotes an enhanced translocation of DAPI molecules through rPanx1 channel. Free energy profiles (ΔG, in kcal/mol) of DAPI translocation across the Panx1 channel pore obtained from the extracellular water (left) to the intracellular side of the channel (right). Profiles were obtained using the Jarzynski equality over eight SMD replicas. Blue color is depicting the free energy profile for rPanx1, while the rPanx1Ser394Phos profile appears in green. The selectivity filter zone is represented as a red bar. ATP pulling direction is shown with a red arrow.

Table S1. Sequences of alanine and aspartate mutants of potential CaMKII phosphorylatable sites in rPanx1.

Mutation	DNA segment	Protein segment
rPanx1	CCCATGTCCCTACAG	DGKVPMSLQTKGE
rPanx1 S384A	CCCATGGCCCTACAG	DGKVPMALQTKGE
rPanx1	CAGGGCAGCCAGAGA	KGEDQGSQRMDFK
rPanx1 S394A	CAGGGCGCCCAGAGA	KGEDQGAQRMDFK
rPanx1	CAGGGCAGCCAGAGA	KGEDQGSQRMDFK
rPanx1 S394D	CAGGGCGACCAGAGA	KGEDQGDQRMDFK

Table S2. Nucleotide sequences of PCR primers used to perform site-directed mutations of amino acid residues of rPanx1.

Mutation	Primers
S384A	Forward GTCCCCATG**GCC**CTACAGAC Reverse TTTTCCATCAATGACGTCCATCT
S394A	Forward ACCAGGGC**GCC**CAGAGAATG Reverse CCTCTCCCTTGGTCTGTAGGGACAT
S394D	Forward ACCAGGGC**GAC**CAGAGAATG Reverse CCTCTCCCTTGGTCTGTAGGGA

Movie S1. Intracellular ATP released through a lateral tunnel of a phosphorylated rPanx1 channel. Steered Molecular Dynamics (SMD) method to pull an ATP molecule from the intracellular side towards the inner cavity of rPanx1S394Phos through a lateral tunnel, and then from the channel cavity towards the extracellular side.

Movie S2. Uptake of DAPI from the extracellular compartment through a phosphorylated rPanx1 channel. Steered Molecular Dynamics (SMD) method to pull a DAPI molecule from the extracellular side towards the inner cavity of rPanx1S394Phos, and then from the channel cavity towards the intracellular side.